Nuclear Instruments and Methods in Physics Research A 612 (2010) 360–366

Contents lists available at ScienceDirect

Nuclear Instruments and Methods in Physics Research A

journal homepage: www.elsevier.com/locate/nima

^{60}Co γ-irradiation effects on electrical properties of a rectifying diode based on a novel macrocyclic Zn octaamide complex

Y.S. Ocak [a], T. Kılıçoğlu [b,c,*], G. Topal [d], M.H. Başkan [e]

[a] Department of Science, Faculty of Education, University of Dicle, Diyarbakir, Turkey
[b] Department of Physics, Faculty of Art & Science, University of Batman, Batman, Turkey
[c] Department of Physics, Faculty of Art & Science, University of Dicle, Diyarbakir, Turkey
[d] Department of Chemistry, Faculty of Education, University of Dicle, Diyarbakir, Turkey
[e] Department of Physics, Faculty of Education, University of Dicle, Diyarbakir, Turkey

ARTICLE INFO

Article history:
Received 30 June 2009
Received in revised form
31 October 2009
Accepted 2 November 2009
Available online 10 November 2009

Keywords:
Rectifying diode
Barrier height
γ-irradiation
Macrocyclic complex
Octaamide

ABSTRACT

$C_{36}H_{28}N_{12}O_8ZnCl_2 \cdot 9/2H_2O$, Zn-octaamide (ZnOA) macrocyclic compound was synthesized to be used in the fabrication of electronic and photoelectronic devices. The structure of new compound was identified by using ^{1}H NMR, ^{13}C NMR, IR, UV–vis and LC–MS spectroscopic methods. The Sn/ZnOA/n-Si/Au structure was engineered by forming a thin macrocyclic organic compound layer on n-Si inorganic substrate and then by evaporating Sn metal on the organic layer. It was seen that the device had a good rectifying behaviour and showed Schottky diode properties. The diode was irradiated under ^{60}Co γ-source at room temperature. Characteristic parameters of the diode were determined from its current–voltage (I–V) and capacitance voltage (C–V) measurements before and after irradiation. It was observed that γ-irradiation had clear effects on I–V and C–V properties. Also, it was seen that the barrier height, the ideality factor and the series resistance values decreased after the applied radiation, while the saturation current value increased.

1. Introduction

Conjugated organic materials have been extensively studied as semiconductors in the applications of electrical and photoelectrical technology. Electronic devices based on these materials have been of interest because of their variability and low cost and easy preparation techniques. It is possible to obtain many electronic and photoelectronic devices by using organic–organic [1–4] and organic–inorganic (OI) structures [5–15]. Many authors have chosen to fabricate OI devices to benefit from the advantages of both materials in a single device [5–15]. OI structures have been used as solar cells [5–8], light emitting diodes [9–10], Schottky diodes [11–19], etc. It is also useful to use organic compounds to understand electrical and optoelectronic properties of them by forming their thin films on well-known inorganic materials. Furthermore, some authors have preferred to use organic compounds as interfacial layers to control electrical properties of metal–semiconductor (MS) diodes [11–24].

Heeger [25] has explained that conjugated polymers can be doped by several methods. One of them is charge injection at a metal–semiconductor polymer interface. Electrons and holes can be injected from metallic contacts into the π*- and π-bands in conjugated compounds, respectively. In this method, organic compounds can be used as an active layer in thin film diodes. Another one is regional oxidation and reduction in semiconducting compounds because of photoabsorption and charge separation. Thus, organic compound layer at metal–semiconductor interface can be useful in the usage of organic compounds in the electrical and photoelectrical devices. In addition, irradiation of conjugated structures may cause to severe effects on the semiconducting properties of conjugated compounds in these devices.

It is well-known that electrical properties of MS and metal–interlayer–semiconductor (MIS) diodes are very sensitive to interface quality. In addition, any mechanism which influences the interface can alter the performance of the device. The effects of gamma irradiation on the electrical and photoelectrical properties of the diodes are of both technological and scientific importances [24]. Recently, some authors have studied the gamma irradiation dose on electrical properties of MS and MIS structures [23,26–29]. In general, transient effects which are caused by electron and hole generation and, permanent effects which cause alters in the crystal structure have been considered [23,26–29]. Some authors have reported increasing and

* Corresponding author at: Department of Physics, Faculty of Art & Science, University of Batman, Batman, Turkey.
E-mail addresses: kilicoglutahsin@gmail.com, tahsin.kilicoglu@batman.edu.tr (T. Kılıçoğlu).

0168-9002/$ - see front matter © 2009 Elsevier B.V. All rights reserved.
doi:10.1016/j.nima.2009.11.008

decreasing effects of any radiation on the barrier height in the devices [23,26–29].

The growth in the application fields of bioorganic, bioinorganic and macrocyclic chemistry has increased the interest on synthesizing new macrocyclic organometal complexes [30]. One of these application fields is electronic and optoelectronic devices such as diodes [15], biosensors [31] and solar cells [32]. Different macrocyclic ligands contain phthalocyanines, porphyrins and pridin units and some metal complexes of different dyes contain thiophene and/or pyridine rings can be shown as examples of compounds used in the applications of electronic and optoelectronic technology [15,33–35]. The common property of these argonometalic complex ligands is having a number of conjugated double bonds.

In this study, the conjugated ZnOA compound was synthesized in order to that it can be used in the fabrication of OI semiconductor device. After synthesizing, it was used for forming organic thin film on inorganic semiconductor substrate. By this way the Sn/ZnOA/n-Si rectifying contact was developed. To see the γ-induced changes on electrical properties of the device, current–voltage (I–V), capacitance–voltage (C–V), conductance–voltage (G–V) and series resistance–voltage (R_s–V) measurements of it were performed before and after irradiation.

2. Experimental procedures

2.1. Synthesis of the Zn complex of 1,3,5,10,12,14,19,21,23,28,30,32-dodeca-aza-2,4:11,13:20,22:29,31-tetrabenzo-cyclohexatricontane-6,9,15,18,24,27,33,36-octaon-cis-7,16,25,34-tetraen ($C_{36}H_{28}N_{12}O_8ZnCl_2)\cdot(9/2H_2O$) (ZnOA)

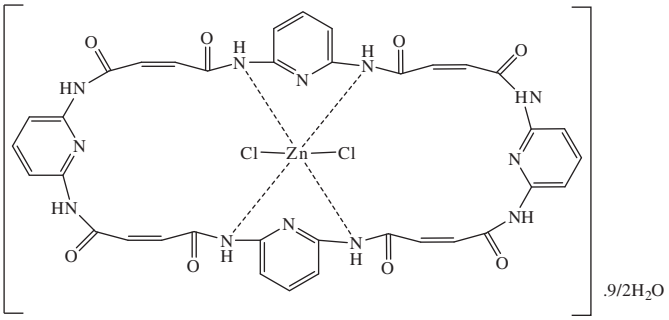

Fig. 1. Molecular structure of $C_{36}H_{28}N_{12}O_8ZnCl_2$ (ZnOA) macrocyclic compound.

All solvents and chemicals used were of analytical reagent grade. $ZnCl_2\cdot4H_2O$ was used as analytical chemical. Maleic acid and 2,6-diaminopyridine were purified before being used. The reaction was carried out in a 1:2:2 molar ratio. A weighed amount of $ZnCl_2\cdot4H_2O$ (2.01 g, 9.7 mmol) was dissolved in methanol (25 ml) at 0 °C in 100 ml two necked round-bottomed flask equipped with a condenser and a dropping funnel and the flask was placed in a magnetic stirrer in an ice-bath. 2,6-diaminopyridine solution in methanol (25 ml) was added dropwise to the stirred solution of $ZnCl_2\cdot4H_2O$. Then solution of maleic acid in methanol (25 ml) was added to reaction mixture without dropping. The reaction mixture was stirred continuously for 16–20 h. The resultant purple crystalline solid product was filtered, washed several times with methanol and dried in air. The compounds were recrystallized in benzene:methanol (1:1) and dried in vacuum. Yield: 1.6 g (96%) mp 164–166 °C. The molecular structure of ZnOA is given in Fig. 1.

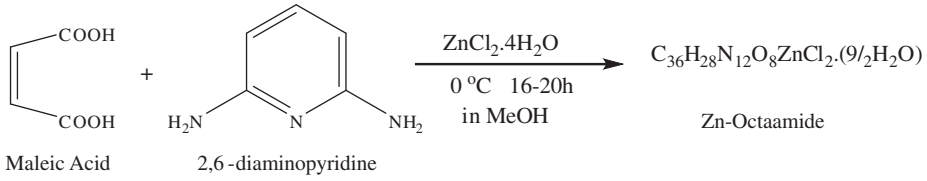

2.2. Physical properties of ZnOA

The UV–vis spectrum of the ZnOA compound in methanol solution was recorded by Perkin Elmer λ-35 UV-Spectrophotometer. The UV-spectrum is presented in Fig. 2a. The IR-spectrum was taken in the 4000–400 cm^{-1} range by using KBr pellet technique with Mattson 1000 spectrophotometer. The IR results are given in Table 1. ^1H NMR measurement was recorded by Bruker AC 400 MHz Spectrometer in $CDCl_3$. ^{13}C NMR measurement was recorded at 200 MHz. The molecular weight of the complex was determined by using Agilent 1100 MSD Spectrometer.

The results of spectral analysis are given as below.

Electronic spectrum of this complex gives two absorption bands in the regions 390–425 (λ_{max}=413.64 nm) and 430–450 nm (λ_{max}=435.25 nm). The optical band gap value of the ZnOA was obtained from its absorption measurement by plotting $(Ahv)^2$ vs. hv graph. The extrapolated value of the optical band gap, E_g, was calculated as 2.79 eV for ZnOA by using Fig 2b.

Characteristics IR bonds (cm^{-1}): 3447, 3403, 3333, 3184, 2866, 1733, 1657, 1580, 1496, 1394, 1317, 1186, 1024, 984, 868, 747, 561. The IR spectrum of the complex derived from 2,6-diaminopyridine shows no change in the pyridine ring which confirms that the nitrogen in the ring do not participate in the coordination. It is well-known that this kind of Zn complexes give octahedral geometry [16,28,34].

^1H NMR spectra (in DMSO) δ(ppm): 5.88 (d, 8H, J=8 Hz), 6.08 (s, 8H), 7.07(bs, 8H), 7.47(t, 4H, J=8 Hz).

^{13}C NMR spectra (in DMSO) δ(ppm): 95.49, 136.15, 145.13, 152.86, 167.84.

MS: the mass spectrum of the complex shows the molecular ion peaks at m/z 893 $[C_{36}H_{28}N_{12}O_8ZnCl_2]^+$ and m/z 976 $[M]^+$+9/2H_2O, μ_{eff}=1.67 B.M.

2.3. Fabrication of Sn/ZnOA/n-Si/Au structure

In this experiment, an n-type Si wafer with (1 0 0) orientation and 1–10 Ωcm resistivity is used for the fabrication of Sn/ZnOA/n-Si/Au structure. The wafer was boiled in 3-choloroethylene and rinsed in acetone and isopropanol by ultrasonic vibration to degrease the wafer. Then it was etched by H_2O/HF (10:1) solution. Preceding each step, the wafer was rinsed in high resistive deionized water. Before inserting into vacuum chamber, cleaned

n-Si semiconductor was dried under N_2. The low resistive ohmic back contact was formed by sputtering of 250 nm Au, followed by a temperature treatment at 450 °C for 15 min in N_2 atmosphere. Before forming a thin ZnOA layer on the n-Si substrate, the native oxide layer on the wafer was removed by H_2O/HF (10:1) solution and it was dried under N_2 atmosphere again. Organic compound layer on n-Si substrate was formed by dipping the substrate in ZnOA solution of 1×10^{-3} mol L^{-1} in methanol. After the formation of the ZnOA layer, Sn metal was evaporated through a shadow mask in the vacuum system by e-beam technique. The evaporation process was carried out at 3×10^{-6} Torr. The diameter of circular diodes was 1 mm. The diode was irradiated under ^{60}Co γ-source an hour. The *I–V* measurements of the device were performed by Keithley 617 electrometer and the *C–V*, *G–V* and R_s–*V* measurements of the device were performed by using Agilent HP 4294A impedance analyzer (40 Hz–110 MHz) before and after irradiation at room temperature. Experimental set-up for electrical measurements of the Sn/ZnOA/n-Si Schottky device is presented in Fig. 3.

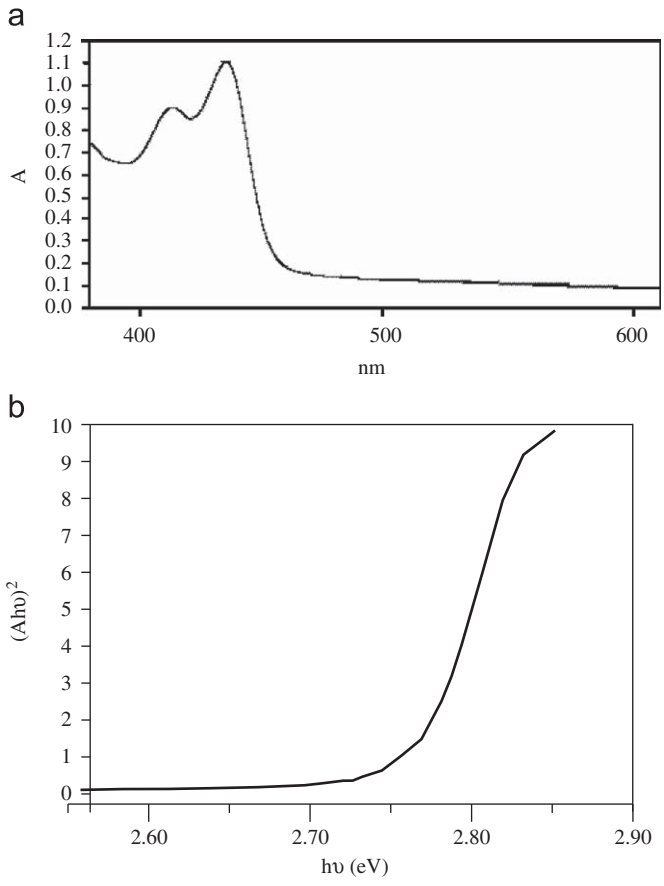

Fig. 2. (a) UV–vis spectroscopy and (b) $(Ahv)^2$ vs. *hv* graph of ZnOA macrocyclic complex.

3. Results and discussion

3.1. Current–voltage characteristics of Sn/ZnOA/n-Si

Fig. 4 shows ln *I–V* plots of Sn/ZnOA/n-Si structure before and after gamma irradiation. As it is shown in the figure both plots have rectifying behaviour. The rectification ratios of *I–V* curves before and after irradiation were calculated as 17,644 and 39,772 between −1 and 1 V, respectively. In addition, the forward and reverse bias currents were significantly increased after irradiation. Thus, γ-irradiation had a clear effect on *I–V* characteristics of the device. When a structure has rectifying behaviour, thermionic emission theory can be taken into account. According to the theory, net current is written as [37,38]

$$I = I_0\left[\exp\left(\frac{qV}{nkT}\right) - 1\right] \quad (1)$$

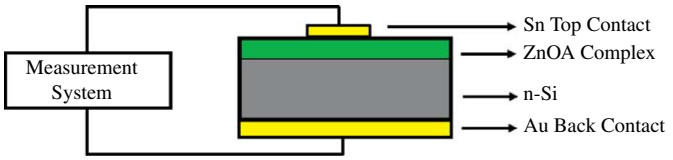

Fig. 3. Experimental set-up for electrical measurements of the Sn/ZnOA/n-Si Schottky device.

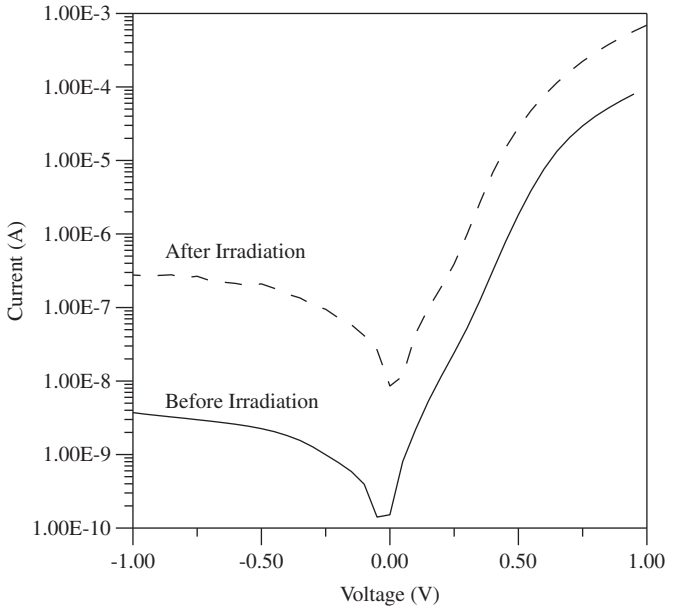

Fig. 4. Current–voltage (*I–V*) measurements of Sn/ZnOA/n-Si diode before and after irradiation.

Table 1
Characteristic IR stretching bonds (cm^{-1}) of ZnOA in KBr pellet.

v(H_2O)	*v*(N–H)	*v*(C–H) oleophilic	*v*(Ar–C–H)	*v*(H_2O) hydrogen bonding	*v*(C═N)	*v*(Ar–C═C)	*Amide*				*v*(N–Zn)
							I	II	III	IV	
3447w	3333s	3277m	3184s 3141vw	2860m,b	1660m	1644m 1496m	1657vs	1580m	1186s	620m	561s

vw: very weak, w: weak, m: medium, s: strong, vs: very strong, b: broad.

where I_0 is the saturation current and expressed as

$$I_0 = AA^*T^2 \exp\left(-\frac{q\phi_b}{kT}\right) \quad (2)$$

where q is the electronic charge, V the applied voltage, k the Boltzmann constant, T the absolute temperature, A the diode area, A^* Richardson constant equals to 110 A cm^{-2} K^{-2} for n-Si [38], n the ideality factor and ϕ_b the barrier height of the diode.

The ideality factor value of the device can be determined from the slope of ln I–V curve of the device by using equation through

$$n = \frac{q}{kT}\frac{dV}{d\ln(I)} \quad (3)$$

and ϕ_b is calculated by using I_0 value determined from the intercept of ln I–V plot on I axis by using the equation given as

$$\phi_b = \frac{kT}{q}\ln\left(\frac{AA^*T^2}{I_0}\right) \quad (4)$$

Table 2 shows n, ϕ_b, I_0 and series resistance (R_s) values determined from I–V characteristics of Sn/ZnOA/n-Si structure. As it is seen in the table, the barrier height of the structure decreased from 0.85 to 0.77 eV. Recently, the increase in barrier height from 0.75 to 0.77 eV for Sn/p-Si diode after irradiation has been reported [28]. Therefore, it can be said that the macrocyclic complex layer between MS has important effects on electrical parameters of the structure and the decrease in the barrier height may be attributed to the increase of free carrier concentration because of regional oxidation and reduction in semiconducting compounds after irradiation. Some authors have found reverse results for MIS structures. For instance, Güllü et al. [23] found an increase in those values for the Al/methyl violet/p-Si Schottky diode from 0.79 to 0.84 eV. They attributed this result to decrease in the carrier concentration in the depletion region of Al/methyl violet/p-Si structure through the occurrence of traps and recombination centers associated with radiation damage.

The ideality factor of the structure decreased from 2.65 to 2.37 after irradiation. The ideality factor which is greater than unity shows the deviation from ideal diode properties and can be attributed to barrier height inhomogenity. To get more information about current mechanisms of irradiated MIS diode, saturation currents were calculated as 0.42 and 7.92 nA before and after irradiation, respectively. Thus it can be easily said that the gamma irradiation increased the generation of free carriers and had a role play in I–V characteristics of the device. The physics of the mechanisms concerning the interaction between the radiation and materials may be summarized as follows. ^{60}Co gamma irradiation breaks of the weakly metal–ligand bond electrons and then leaved free electrons flow from Zn to N atoms which are in amide groups. Hereby, holes are formed on Zn atom and then Zn is locally reduced. Because of the electron flow from metal to N atoms, the electron density on ligand atoms are increased and then ligand is oxidized. Thus, local reduction and oxidation in complex structure cause the increase of the free carrier density between the metal and inorganic semiconductor.

It is known that there is always a downward concave curvature in forward bias I–V plots of rectifying diodes because of the R_s. Cheung's method [39] can be used to calculate the parameters of Sn/ZnOA/n-Si Schottky diode. Cheung's functions has been defined as

$$\frac{dV}{(d/\ln I)} = IR_s + n\left(\frac{kT}{q}\right) \quad (5)$$

$$H(I) = V - n\left(\frac{kT}{q}\right)\ln\left(\frac{I}{AAT^2}\right) = IR_s + n\phi_b \quad (6)$$

The $dV/d\ln I$–I and $H(I)$–I plots of the device before and after irradiation are shown in Figs. 5 and 6. The slopes and y-axis intercepts of given $dV/d\ln I$–I plots give R_s and nkT/q values by using Eq. (5), respectively. The values of R_s and n for unirradiated diode were calculated as 2.5 kΩ and 2.62. They were found as 0.5 kΩ and 2.5 after radiation applied. Therefore, there is a good coherence between the values of n obtained from both ln I–V and $dV/d\ln I$–I plots. Furthermore, a severe effect of radiation on R_s is seen. The plots of $H(I)$–I give straight lines whose y-axis intercepts equal to barrier heights. The consistency of the method can be checked from the slopes of the plots given R_s values. Using $H(I)$–I plots by the help of Eq. (6), ϕ_b and R_s values were determined as 0.85 eV and 2.4 kΩ before irradiation and 0.76 eV and 0.49 kΩ after irradiation. The results obtained from both $dV/d\ln I$–I and $H(I)$–I plots are in consistency with each other.

Comparing R_s and ϕ_b values obtained from another method could be very useful. Norde has claimed an alternative approach to calculate these values from I–V data. The following equation has been defined to analyze I–V measurements [40,41]:

$$F(V) = \frac{V}{\gamma} - \frac{kT}{q}\left(\frac{I(V)}{AA^*T^2}\right) \quad (7)$$

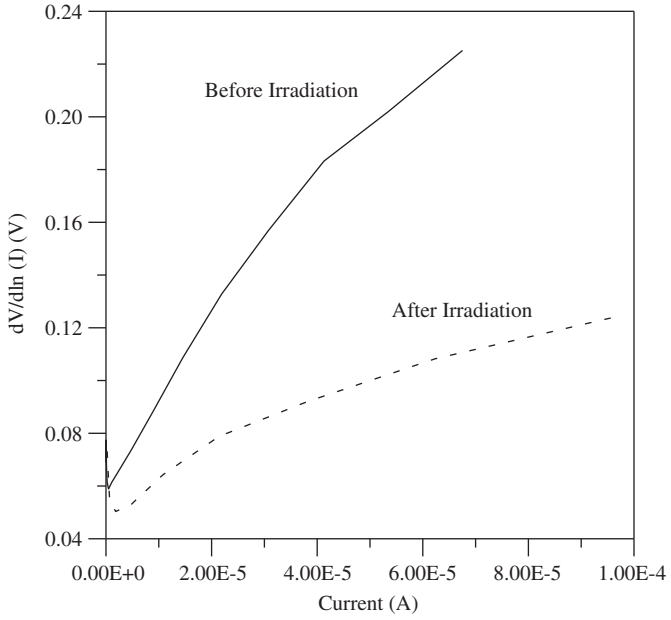

Fig. 5. $dV/d\ln(I)$–V plots of Sn/ZnOA/n-Si diode obtained from its forward bias I–V measurements before and after irradiation.

Table 2
Some electrical parameters obtained from forward I–V measurements of Sn/ZnOA/n-Si diode before and after irradiation.

	I–V			$dV/d\ln I$		H(I)–I		Norde	
	ϕ_b (ev)	n	I_0 (nA)	n	R_s (Ω)	ϕ_b (ev)	R_s (Ω)	ϕ_b (ev)	R_s (Ω)
Before irradiation	0.85	2.65	0.42	2.62	2530	0.85	2365	1.00	1422
After irradiation	0.77	2.37	7.92	2.5	499	0.76	485	0.85	1097

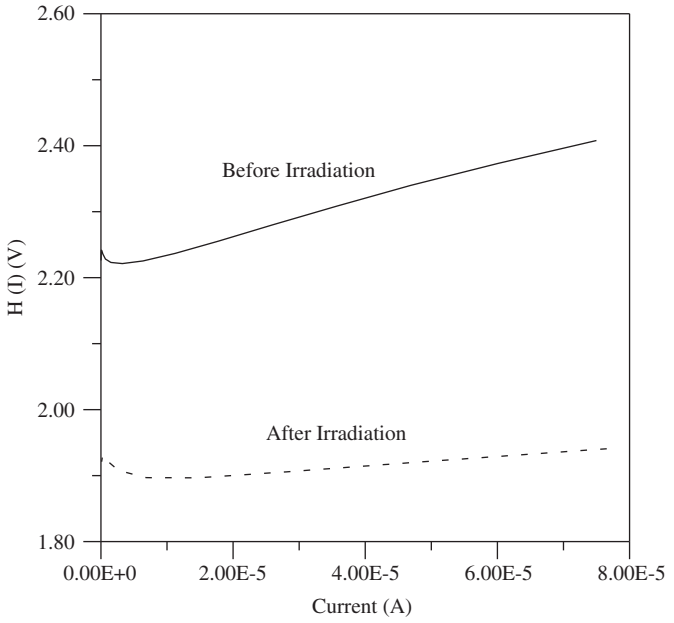

Fig. 6. *H(I)–I* plots of the diode obtained from its forward bias *I–V* measurements before and after irradiation.

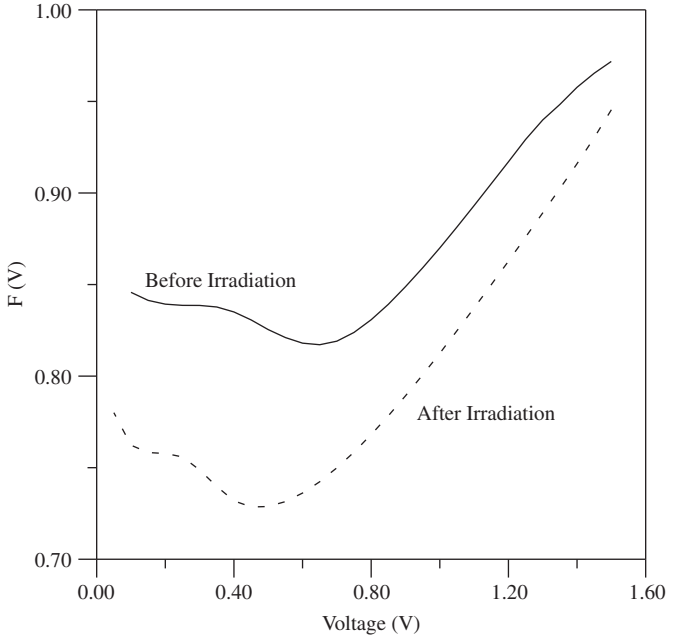

Fig. 7. *F(V)–V* plots of the diode before and after irradiation.

where γ is a the first integer greater than n and $I(V)$ is the current obtained from the *I–V* curve. In this study γ has been taken as 3. The barrier height of device can be obtained by using [41]

$$\phi_b = F(V_0) + \frac{V_0}{\gamma} - \frac{kT}{q} \tag{8}$$

where $F(V_0)$ is the minimum $F(V)$ value of F vs. V graph and V_0 is the corresponding voltage. Fig. 7 shows the $F(V)$–V graph of the Sn/ZnOA/n-Si diode. The R_s can be calculated through the relation [41]

$$R_s = \frac{kT(\gamma - n)}{qI} \tag{9}$$

The values of R_s and ϕ_b for the diode were calculated as 1.4 kΩ and 1.00 eV for unirradiated, and as 1 kΩ and 0.85 eV for irradiated case, respectively. It is also very clear that R_s and ϕ_b values determined from both methods were decreased by irradiation.

3.2. Capacitance–voltage, conductance–voltage and series resistance–voltage characteristics of Sn/ZnOA/n-Si

The *C–V* measurements of Sn/ZnOA/n-Si structure were performed at 500 kHz for the diode before and after irradiation. The depletion layer capacitance is given as follows [40]:

$$\frac{1}{C^2} = \frac{2(V_0 + V)}{q\varepsilon_s A^2 N_D} \tag{10}$$

where A is the effective diode area, ε_s the dielectric constant of semiconductor, V the applied reverse bias and V_0 the diffusion potential at zero bias determined from the extrapolation of the linear reverse bias C^{-2}–V plot to the V axis. Fig. 8 presents the irradiated and unirradiated C^{-2}–V plots of the structure at 500 kHz. The ϕ_b value can be determined from following well-known equation:

$$\phi_{b_{(C-V)}} = V_0 + V_p \tag{11}$$

where V_p is the potential difference between the bottom of the conduction band in the neutral region of n-Si and Fermi level and can be determined if the carrier concentration N_D is known. The value of V_p has been calculated as 0.257 eV. The ϕ_b values of the diode have been determined using Eq. (11) as 0.98 and 0.88 eV before and after irradiation process, respectively. So, the results obtained from both *I–V* and *C–V* characteristics are consistent with each other.

In addition, the conductance values depend on several parameters including the thickness and nature of interlayer between metal and semiconductor, series resistance and interface state density [40]. The influence of interface state density can be eliminated if the *G–V* measurements are carried out at sufficiently high frequencies [37,33–45], because the charges at the interface cannot follow an ac signal [43]. Fig. 9a and b shows unirradiated and irradiated *G–V* measurements of the structure at different

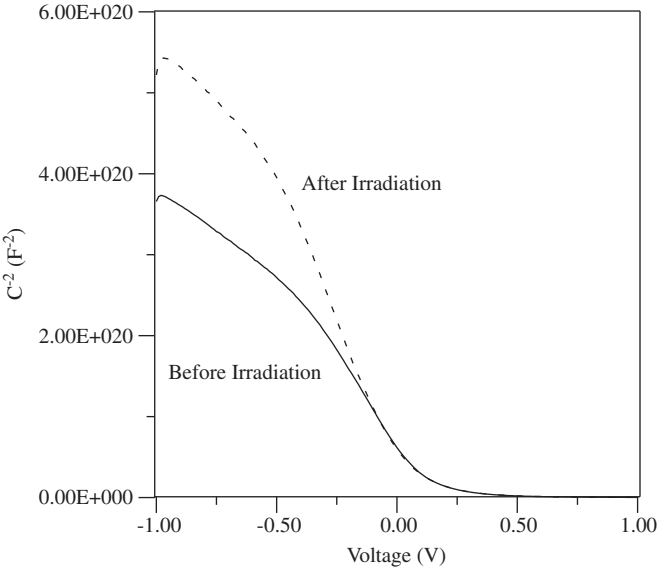

Fig. 8. C^{-2}–V plots of Sn/ZnOA/n-Si diode before and after irradiation.

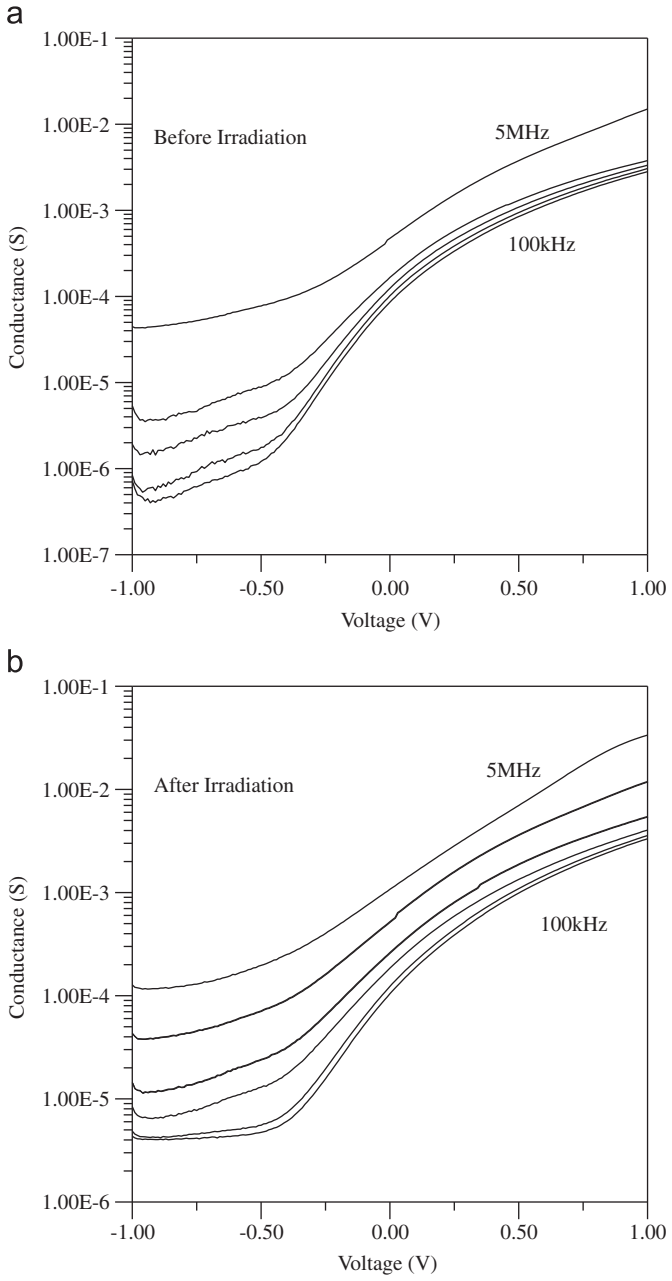

Fig. 9. Forward and reverse bias conductance–voltage (G–V) measurements of Sn/ZnOA/n-Si diode (a) before and (b) after irradiation at different frequencies.

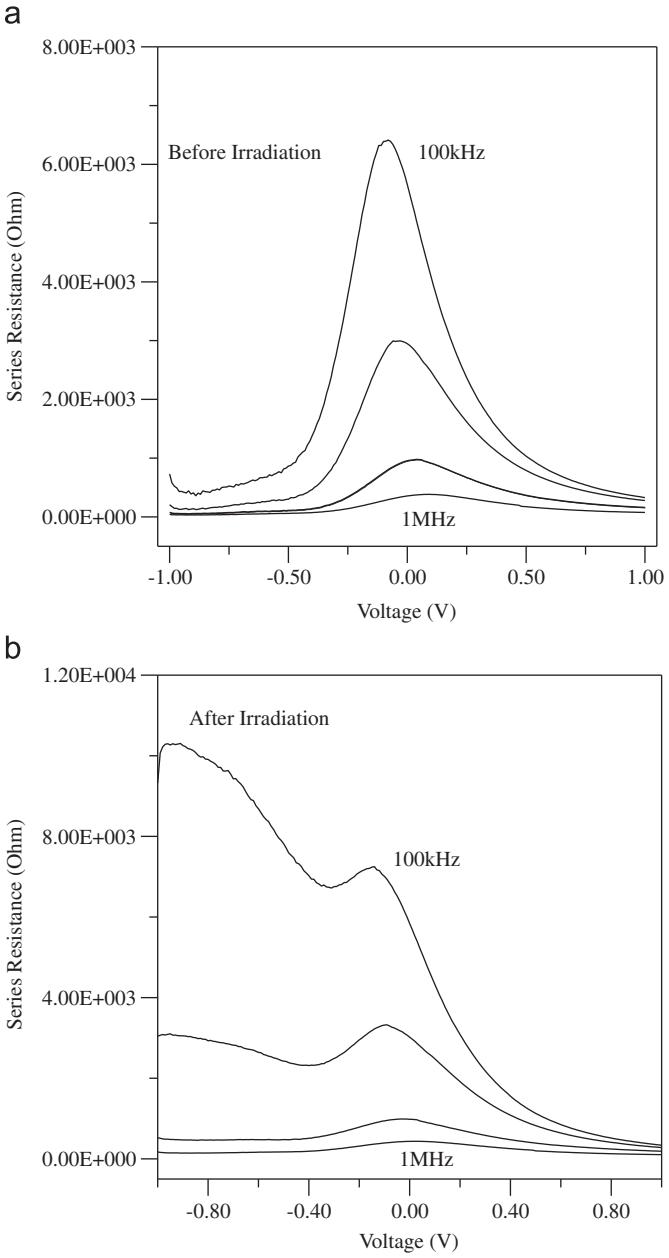

Fig. 10. Forward and reverse bias series resistance–voltage (R_s–V) measurements of Sn/ZnOA/n-Si diode (a) before and (b) after irradiation at different frequencies.

frequencies, respectively. As it is shown in the figures, at high frequencies, there is no significant effect of irradiation on conductance properties of the structure. However, at low frequencies such as 100 kHz the reverse bias conductance values increase and the reverse bias conductance plots are more saturated than unirradiated ones. These parameters show the severe effects of γ-irradiation on interface state density, therefore on conductivity of the diode.

Furthermore, the series R_s–V measurements of the diode are given in Fig. 10a and b. The peaks at high frequencies are related to interface states. As it is seen in Fig. 10a, the peak intensity is decreased when frequency is increased. It can be said that interface states cannot follow fast alternating current (ac) signal at high frequencies. After irradiation, the peak intensity starts to disappear and reverse biased R_s values start to increase (Fig 10b).

4. Conclusion

In this study, a conjugated ZnOA compound was synthesized to use it in semiconductor applications. After identifying the complex, it was used in the fabrication of Sn/ZnOA/n-Si/Au structure. The structure had rectifying behaviour. The characteristic parameters of the diode were determined before and after gamma irradiation. It was seen that unlike saturation current, the barrier height, the ideality factor and the series resistance values of the device decreased after the applied radiation. This situation

can be attributed to increase of free carriers of the macrocyclic compound between metal and the inorganic semiconductor after gamma irradiation.

Acknowledgement

This work was supported by Grant no. 06-FF-81 of the Research Fund of University of Dicle (DÜBAP).

References

[1] C.W. Tang, S.A. VanKlyke, Appl. Phys. Lett. 51 (1987) 913.
[2] X. Jiang, Z. Zhang, W. Zhao, W. Zhu, B. Zhang, S. Xu, J. Phys. D: Appl. Phys. 33 (2000) 473.
[3] J. Brabec, N.S. Sariciftci, J.C. Hummelen, Adv. Funct. Mater. 11 (1) (2001) 15.
[4] H. Mu, H. Shen, D. Klotzkin, Solid-State Electron. 48 (10–11) (2004) 2085.
[5] B. O'Regan, M. Gratzel, Nature 353 (1991) 737.
[6] K. Ocakoğlu, F. Yakuphanoğlu, J.R. Durrant, S. İçli, Sol. Energy Mater. Sol. Cells 92 (2008) 1047.
[7] Ö. Güllü, A. Türüt, Sol. Energy Mater. Sol. Cells 92 (2008) 1205.
[8] M.M. El-Nahass, H.M. Zeyada, K.F. Abd-El-Rahman, A.A.A. Darwish, Sol. Energy Mater. Sol. Cells 91 (2008) 1120.
[9] N.D. Kumar, M.P. Joshi, C.S. Friend, P.N. Prasad, R. Burzynski, Appl. Phys. Lett. 71 (1997) 1388.
[10] S. Guha, R.A. Haight, N.A. Bojarczuk, D.W. Kisker, J. Appl. Phys. 82 (1997) 4126.
[11] R.K. Gupta, R.A. Singh, J. Polym. Res. 11 (2004) 269.
[12] R.K. Gupta, K. Ghosh, P.K. Kahol, Curr. Appl. Phys. 9 (2009) 933.
[13] A. Ashery, A.A.M. Farag, M.A. Salem, Microelectron. Eng. 85 (2008) 2309.
[14] A.R.V. Roberts, D.A. Evans, Appl. Phys. Lett. 86 (2005) 072105.
[15] F. Yakuphanoğlu, M. Kandaz, B.F. Senkal, Thin Solid Films 516 (2008) 8793.
[16] T. Kılıçoğlu, Thin Solid Films 516 (2008) 967.
[17] T. Kılıçoğlu, M.E. Aydın, Y.S. Ocak, Physica B 388 (2007) 244.
[18] T. Kılıçoğlu, M.E. Aydın, G. Topal, M.A. Ebeoğlu, H. Sayğılı, Synth. Met. 157 (2007) 540.
[19] K. Akkılıç, Y.S. Ocak, S. İlhan, T. Kılıçoğlu, Synth. Met. 158 (2008) 969.
[20] K. Akkılıç, İ. Uzun, T. Kılıçoğlu, Synth. Met. 157 (2007) 297.
[21] Ş. Aydoğan, M. Sağlam, A. Türüt, Y. Onganer, Mater. Sci. Eng.: C 29 (2009) 1486.
[22] Ö. Güllü, Ö. Barış, M. Biber, A. Türüt, Appl. Surf. Sci. 254 (2008) 3039.
[23] Ö. Güllü, M. Çankaya, M. Biber, A. Türüt, J. Phys. D: Appl. Phys. 41 (2008) 135103.
[24] Z. Ahmad, M.H. Sayyad, Physica E 41 (2009) 631.
[25] A.J. Heeger, Rev. Mod. Phys. 73 (2001) 681.
[26] Ş. Karataş, A. Türüt, Ş. Altındal, Radiat. Phys. Chem. 78 (2009) 130.
[27] A. Tataroğlu, Ş. Altındal, Sensors Actuators A 151 (2009) 168.
[28] Ş. Karataş, A. Türüt, Nucl. Instrum. Methods Phys. Res. A 566 (2006) 584.
[29] P. Jayavel, J. Kumar, K. Santhakumar, P. Magudapathy, K.G.M. Nair, Vacuum 57 (2000) 51.
[30] A. Chaudry, N. Bansal, A. Gajraj, R.V. Singh, J. Inorg. Biochem. 96 (2003) 393.
[31] V. Laurinavicius, J. Razumiene, A. Ramanavicius, A.D. Ryabov, Biosens. Bioelectron. 20 (2004) 1217.
[32] C.Y. Kwong, A.B. Djurisic, P.C. Chui, L.S.M. Lam, W.K. Chan, Appl. Phys. A 77 (2003) 555.
[33] A. Chowdhury, J. Chowdhury, P. Pal, A.J. Pal, Solid State Commun. 107 (1998) 725.
[34] M.Y. Li, S.J. Feng, S.B. Fang, X.R. Xiao, X.P. Li, X.W. Zhou, Y. Lin, Chin. Sci. Bull. 52 (2007) 2320.
[35] D.M. de Leeuw, E.J. Lous, Synth. Met. 65 (1994) 45.
[36] W.U. Malik, R. Bembi, R.D. Singh, Polyhedron 2 (1989) 369.
[37] E.H. Rhoderick, R.H. Willams, Metal–Semiconductor Contacts, Clarendon, Oxford, 1988.
[38] S.M. Sze, K. Ng. Kwok, Physics of Semiconductor Devices, third edition, Wiley, New York, 2007.
[39] S.K. Cheung, N.W. Cheung, Appl. Phys. Lett. 49 (1986) 85.
[40] H. Norde, J. Appl. Phys. 50 (1979) 5052.
[41] Ş. Karataş, S. Altındal, A. Türüt, M. Çakar, Physica B 392 (2007) 43.
[42] E.H. Rhoderick, Metal–Semiconductor Contacts, Oxford University Press, Oxford, 1978.
[43] Ö.F. Yüksel, S.B. Ocak, A.B. Selçuk, Vacuum 82 (2008) 1183.
[44] S. Karadeniz, N. Tuğluoğlu, T. Serin, N. Serin, Appl. Surf. Sci. 246 (2005) 30.
[45] E.H. Nicollian, J.R. Brews, MOS Physics and Technology, Wiley, New York, 1982.